ELSEVIER

Contents lists available at ScienceDirect

Results in Optics

journal homepage: www.sciencedirect.com/journal/results-in-optics



Optical band gap engineering and comparison of conductivity of CaTiO₃ and LiNbO₃ doped PVDF films

Clyde Varner *,1, Angela Davis 1, Ashok K. Batra, Padmaja Guggilla

Department of Physics, Chemistry, and Mathematics, College of Engineering, Technology and Physical Sciences, Alabama A&M University, Normal, AL, USA

ARTICLE INFO

Keywords:
Band Gap Engineering
DC Conductivity
Nanogenerator
Perovskite
Doped

ABSTRACT

This study explores the impact of CaTiO₃ and LiNbO₃ crystals on the optical and dielectric properties of polyvinylidene fluoride (PVDF) films. Our investigation employs UV–Visible Spectroscopy to characterize the n- π * C-F related electronic transition within the PVDF matrix. We find that CaTiO₃ crystals significantly decrease the composite's band gap and dielectric properties, enhancing its electronic and optical attributes. Conversely, LiNbO₃ crystals increase the band gap energy. These variations align with observed DC conductivity changes, suggesting novel functionalities for optoelectronic, sensing, and energy storage applications.

1. Introduction

The exploration of nanomaterials in materials science represents a pivotal shift towards engineering advanced materials with unprecedented capabilities. Nanomaterials, characterized by their nanoscale dimensions, exhibit unique physical, chemical, and electrical properties that diverge significantly from their bulk counterparts, due to the quantum size effect and increased surface area to volume ratio. This has opened up new frontiers in materials engineering, enabling the development of materials with tailored properties for specific applications (Zhang et al., 2023; Abbas et al., 2023; Omeiza et al., 2023). Recent studies have highlighted the use of perovskites for optoelectronic devices and solid-state lighting (Chahar et al., 2024; Advanced Materials for Solid State Lighting, 2023). Specifically, the use of nanostructured materials such as CaTiO3 and LiNbO3 has been at the forefront of innovations in fields ranging from energy conversion and storage to environmental remediation and healthcare (Chahar et al., 2024; MDPI, 2023; Cerda-Sumbarda et al., 2023). CaTiO₃, for instance, is notable for its luminescent and photocatalytic properties (Kumar et al., 2023; Mehra, 2022), while LiNbO₃ is not a perovskite, it is recognized for its non-linear optical and piezoelectric characteristics (Kumar et al., 2023). Such properties are key in developing innovative materials for optoelectronic devices (Mehra, 2022; Mallick et al., 2023; Ostlind et al.,

Polyvinylidene Flouride (PVDF) is a semi crystalline per-fluorinated polymer. PVDF is known for its piezoelectric, ferroelectric, and

pyroelectric properties. The integration of these nanocrystals into polymer matrices, such as PVDF, presents a unique opportunity to harness their distinct properties in a flexible and durable form, making them ideal candidates for a wide array of technological applications. This integration not only leverages the intrinsic properties of the nanocrystals but also introduces synergistic effects that can enhance the overall performance of the composite material (Tabhane et al., 2022; Dilshod et al., 2022; Acikgoz et al., 2023; Novruzova, 2021). Through the systematic investigation of these composites, this study aims to contribute to the body of knowledge on material science, focusing on the intricate relationship between nanostructuring and material properties enhancement. By elucidating the mechanisms behind the observed modifications in electronic properties and band gap engineering, this research aspires to pave the way for the next generation of materials science innovations, showcasing the transformative potential of nanomaterials in shaping the future of technology. Xu et al. reported on enhanced dc conductivity in ionic liquid doped PVDF composites (Xu et al., 2017). In this study, we methodically investigate the integration of CaTiO3 and LiNbO3 crystals into a PVDF matrix, focusing on how this affects the n- π * C-F bond PVDF material band gap and dielectric properties. This research seeks to uncover the underlying mechanisms driving these changes and to understand how the unique attributes of these crystals contribute to the altered electronic properties of the PVDF composite (Wu et al., 2022; Jilani et al., 2021; Chaibi et al., 2021; Qahtan et al., 2021; Synak et al., 2022; Tan et al., 2022). The findings are expected to provide valuable insights into band gap engineering and

^{*} Corresponding author.

E-mail address: clyde.varner@aamu.edu (C. Varner).

¹ Both Authors Contributed Equally to this work.

dielectric behavior modification in composite materials used for optoelectronic devices and solid state lighting.

In our study we used UV–Visible spectroscopy to obtain the UV–Vis spectrum of the doped composites and pure PVDF between 2–6 eV. The UV–Vis spectrum was used as the basis to derive other information related to the composites. We calculated the direct and indirect band gap, optical conductivity, dielectric permittivity, refractive and refractive index. The spectrum spectra are very informative and from the optical conductivity spectra we calculated the DC conductivity.

This research not only advances the understanding of dopant-induced modifications in PVDF but also opens up new avenues for the application of these materials in areas like flexible electronics, energy harvesting, and sensor technology. The findings highlight the versatility of PVDF as a host matrix for dopants and its potential in creating materials with customized electrical and optical properties for specific technological applications.

2. Materials and Methods

PVDF (poly vinylidene di fluoride), CaTiO3 (calcium titanite), and LiNbO₃ (lithium niobite) were purchased from sigma Aldrich and used as is. The procedure is modified from existing literature on PVDF polymer using solution casting with dimethyl formamide as a solvent (Xu et al., 2017; Wenzhong Ma Jun Zhang and Wang, 2008; Kunwar et al., 2022). The procedure involves ultrasonic agitation of the PVDF polymer in DMF (dimethyl formamide) solution at 25 deg C for 1 h. To the resultant solution either the appropriate amount of dopant CaTiO3 or LiNbO₃ were used. While keeping the dopant amount the same, we changed the PVDF amounts to give a ratio dopant: PVDF of 6, 9, and 37 wt% respectively. For a film this change in PVDF amount corresponds to a change in thickness of the material. After we evaporate the DMF solvent. Fourier transform infrared spectra (FTIR) in attenuated total refection (ATR) mode were collected using a Thermo Fisher Nicolet in ATR mode with a diamond crystal. For each measurement, 16 scans were performed with a measurement resolution of 2 cm⁻¹. The UV-Vis were taken on a Hitachi U-2900 spectrometer with 10 nm resolution between 200-600 nm. All post processing of the data was done in OriginPro software.

2.1. Uv-Vis spectroscopy analysis

The UV–Vis spectra of both $LiNbO_3$ and $CaTiO_3$ crystals in the PVDF

UV-VIS Lithium Niobate in PVDF 0.27 0.27 0.18 0.09 0.00 0.00 405 Wavelength

Fig. 1. UV-Vis Spectrum of 6, 9, and 38 wt% LiNbO₃: PVDF.

matrix (Figs. 1 and 2, respectively) exhibit distinct characteristics compared to pure PVDF. The concentration of Dopant is kept the same in both cases while only varying the thickness of PVDF Film. Notably, the $n\text{-}\pi^*$ region (~357 nm) of the spectrum of the CaTiO_3-doped PVDF shows a substantial dip and a shift towards lower wavelengths, indicative of a full peak emergence in the spectrum. The UV–Vis plots of the CaTiO_3 and the LiNbO_3 crystals were also taken in solution phase to identify the region of overlap between the CaTiO_3 absorption and the small dip feature in the PVDF spectrum around the $n\text{-}\pi^*$ region. Lithium Niobate did not show any transition here which explains why the similar effect is not observed in the uv–vis spectrum. Additionally, it is interesting to note that the LiNbO_3 samples in PVDF showed an opposite effect where the dip in this region due to PVDF is decreased, showing some altering effects on the electronic structure that is sensitive to these wavelength regions.

2.2. Band gap

The band gap spectra were analyzed using the modified semi-conductor background correction method (Makuła et al., 2018) (Figs. 3 and 4). The behavior, associated with band gap lowering effects, is attributed to the presence of $CaTiO_3$ within the matrix. The band gap spectra reveal a decrease in the energy gap (eV) for the $CaTiO_3$ embedded sample relative to pure PVDF. Conversely, the $LiNbO_3$ doped sample demonstrates an increase in both indirect and direct band gap energies. The specific causes of these band gap modifications are attributed to the unique influences of each dopant within the PVDF matrix

Dielectric Constant: Fig. 5, displays the real component of the CaTiO₃ doped PVDF Dielectric Constant spectra for the real component. The dielectric loss, the imaginary portion of the dielectric constant is shown in Fig. 6, next page, and is representative of the composites ability to store charge. The high dielectric constant and refractive index of the perovskite-type CaTiO₃, combined with the ferroelectric and piezoelectric properties of PVDF (Wang et al., 2020), lead to substantial alterations in the dielectric behavior of the composite. There is a drop to zero for the real component of the permittivity Fig. 5 curves around 3.6 eV. Indicating that the material exhibits unique electromagnetic properties. This point can correspond to a transition from a dielectric behavior to a conductive one. With respect to the real permittivity CaTiO₃ curves, this could indicate an additional resonance condition where the material does not store energy but rather allows the

UV-VIS Calcium Titanate in PVDF

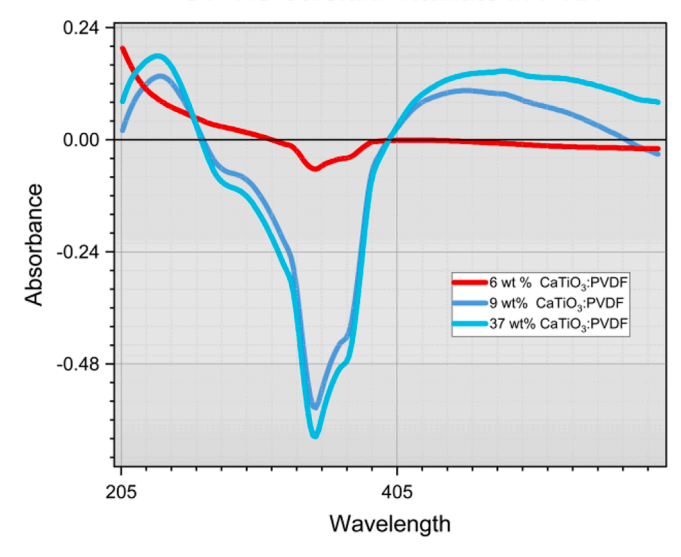


Fig. 2. UV-Vis Spectrum of 6, 9, and 37 wt% CaTiO₃: PVDF.

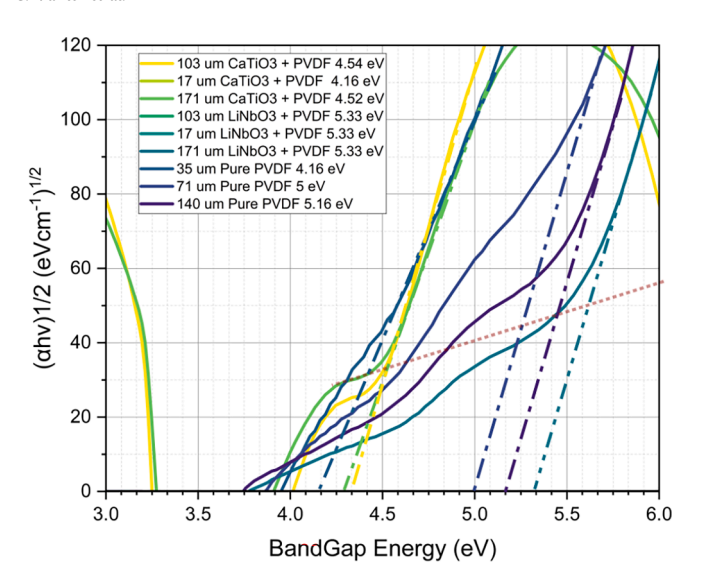


Fig. 3. Indirect Band Gap Calculation for all samples.

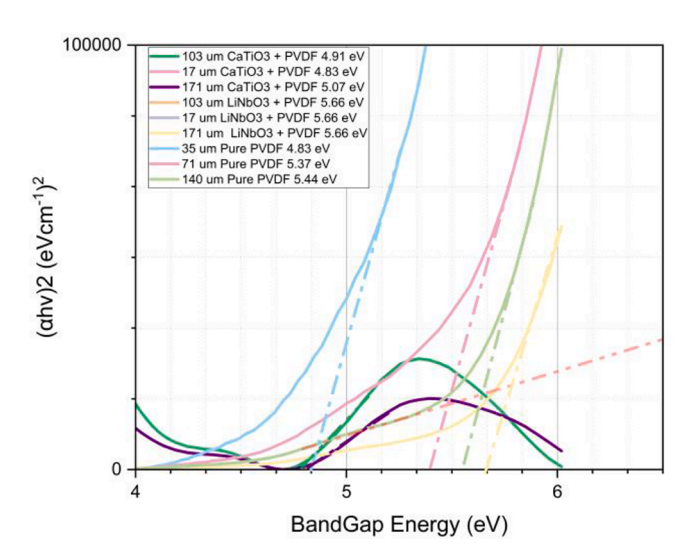
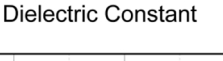


Fig. 4. Direct Band Gap Calculation for all Samples.

electromagnetic wave to pass through with minimal absorption or reflection. The concentrations were chosen to exhibit the linear range of Absorbance vs. wt.% of CaTiO₃: PVDF from 6-9 wt%. We found that after increasing the concentration further from 9 wt% to 37 wt% there was no significant increase in the spectra in this region. Indicating a saturation effect due to percolation. Since a large concentration of CaTiO₃ crystals in close proximity to each other can form conductive pathways, percolation reaches a maximum and does not lead to significant linear increase in the UV–Vis spectrum in Fig. 1. LiNbO₃ samples show a smaller background, indicating a decrease in inter-sub band absorption. This observation is consistent with the increased band gap seen in the UV–Vis analysis of LiNbO₃ (Figs. 3 and 4). The contrast in background intensities between CaTiO₃ (Fig. 7) and LiNbO₃ (Fig. 8) samples in the FTIR spectra provides further evidence of the distinct electronic properties induced by each type of crystal within the PVDF matrix.

Overall, these spectral analyses reveal significant modifications in the optical and dielectric properties of the PVDF matrix upon doping with CaTiO₃ and LiNbO₃ crystals. The observed changes in the band gap, dielectric constant, and other optical properties underscore the potential of these composites for various advanced material applications, including sensors, actuators, and capacitors. The integration of the unique properties of the ceramic components with the flexibility and



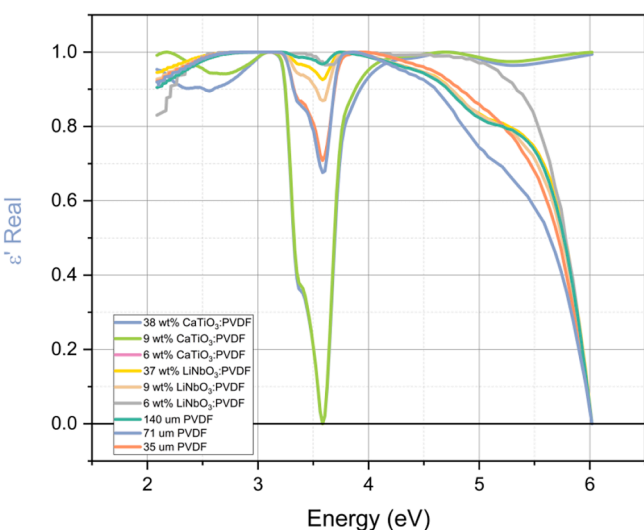
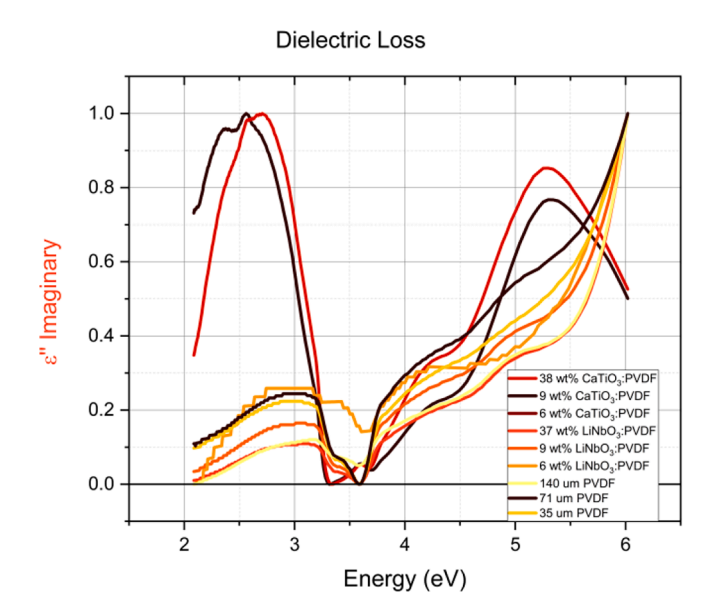


Fig. 5. Real Dielectric Constant Normalized for Comparison.



 $\textbf{Fig. 6.} \ \ \textbf{Imaginary Dielectric Loss normalized for Comparison.}$

strength of PVDF showcases the promise of these composite materials in technological innovations.

Relative DC Conductivity: The relative DC Conductivity of the samples (Table 1, next page) were calculated from extrapolation of the normalized optical conductivity (A4) after fitting to the Drude Model to obtain the value of the optical conductivity at eV = 0 (Mayou, 2000; Neagu et al., 2000). These values are in line with reported PVDF conductivity values in the literature (Xu et al., 2017). The only variance in the weight percent is due to the volume of PVDF added while all dopant amounts remain the same. The DC Conductivities show that as the PVDF amount is decreased (Dopant: PVDF wt.% increase) in the CaTiO₃ sample, the trend in wt.% increase leads to higher DC conduction. A significant enhancement in relative DC conductivity with increasing CaTiO₃ dopant concentration is attributed to the formation of microstructures that facilitate charge transport (Xu et al., 2017). Moreover, the band gap of the PVDF membranes exhibited a noticeable shift, suggesting altered electronic structures due to dopant integration. This shift in band gap points to potential applications in optoelectronic

FTIR Calcium Titanate in PVDF

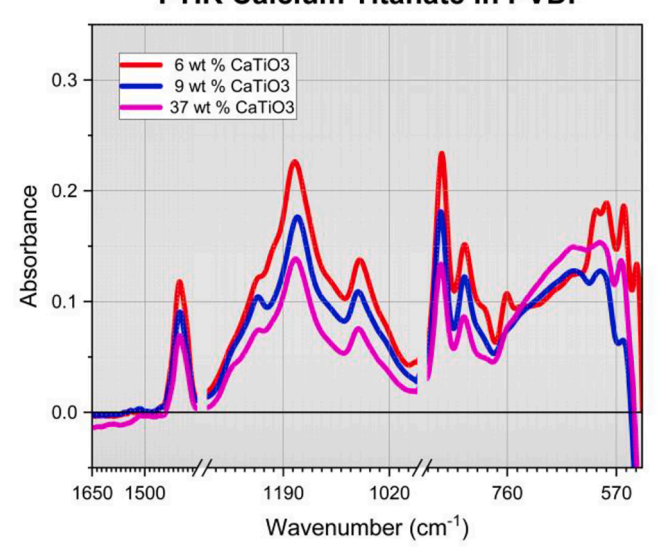


Fig. 7. FTIR Spectrum of CaTiO₃ in PVDF.

FTIR Lithium Niobate in PVDF

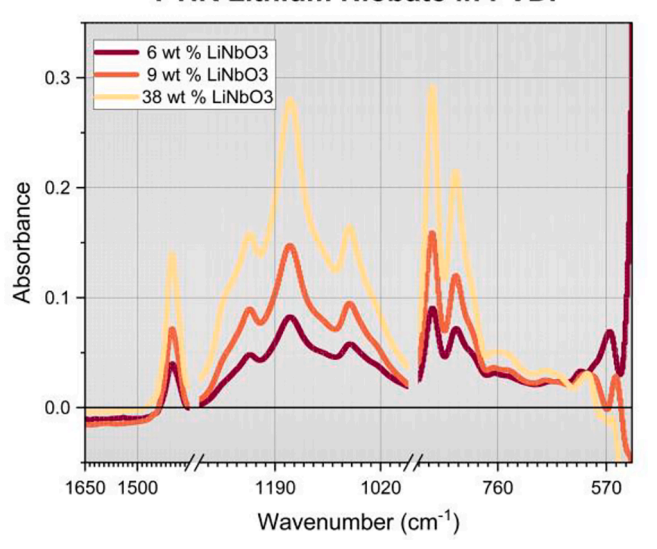


Fig. 8. FTIR Spectrum of LiNbO₃ in PVDF.

devices where tailored band gaps are crucial.

Crystallinity: The samples showed characteristic peaks of α phase, that were observed at 615, 764, 795, and 975 cm $^{-1}$ (Zhou et al., 2021). The β phase was attributed to the peaks at 840, 1276 and 1431 cm $^{-1}$ (Zhou et al., 2021; Zhou and Cakmak, 2007; Uličná et al., 2022; Panda et al., 2022). This observed presence of Beta phase with increase of the

Crystals Dopant seems to follow the effects of conductivity. Following the peak at 840 cm⁻¹, the Beta phase after CaTiO₃ doping (Fig. 7) showing an increase with PVDF Amounts added. The background is very high to the low wavenumber side indicating the presence of Charge Carriers and Specific Peaks related to CaTiO₃. The Beta phase in LiNbO₃ (Fig. 8) shows an increase with decreasing PVDF Amounts added. This means that the presence of Beta Phase is key to the electrical properties of the composite (Panda et al., 2022).

3. Conclusion

Our findings elucidate the complex relationship between CaTiO₃ dopant concentration, PVDF matrix thickness, and the resultant alterations in band gap and dielectric behavior, and DC conductivity; spotlighting the transformative potential of these composite materials in fields as diverse as optoelectronics, sensor technology, and energy storage systems (Omeiza et al., 2023; Advanced Materials for Solid State Lighting, 2023; Cerda-Sumbarda et al., 2023; Kumar et al., 2023; Mehra, 2022; Mallick et al., 2023).

The strategic incorporation of CaTiO₃ and LiNbO₃ crystals into the PVDF matrix has ushered in substantial modifications in electronic and optical properties, pivotal for the advancement of materials science. Notably, the CaTiO₃ doping leads to a nuanced transition from dielectric to conductive behavior, underscored by a marked percolation threshold at approximately 9 % concentration, as revealed through meticulous UV–Vis spectroscopy analysis. This transition, intricately dependent on the matrix thickness, signifies a shift in the material's functionality, enabling the crafting of composites with tailored electrical conductivities (Xu et al., 2017; Wenzhong Ma Jun Zhang and Wang, 2008; Kunwar et al., 2022; Mayou, 2000; Neagu et al., 2000; Chahar et al., 2024; Advanced Materials for Solid State Lighting, 2023). Such precise control over the material's electrical properties opens up new avenues for the design of advanced optoelectronic devices, wherein conductivity can be finely tuned to suit specific application requirements.

Furthermore, the observed minimal increase in the effects with a significant leap in dopant concentration to 37 % (four-fold increase) underscores a critical saturation point, emphasizing the importance of optimizing dopant levels for desired outcomes without redundancy. This also maintains the stretchable properties of the PVDF matrix itself – determining that above 9 % a satuation effect is observed providing a limit needed to create conductive pathways. This insight not only champions the efficient use of resources but also heralds a step-change in the economic fabrication of composite materials, ensuring that each constituent is judiciously utilized to its fullest potential.

In contrast, the unique behavior observed with LiNbO3 doping, which operates to increase the observed band gap in PVDF composites uses the same modulation of the crystalline phases and thereby the electrical and optical properties of PVDF, this result offers a complementary strategy for material design (Xu et al., 2017; Wenzhong Ma Jun Zhang and Wang, 2008; Kunwar et al., 2022). This highlights a distinct avenue for engineering the electronic structure of composite materials, catering to applications that demand lower conductivity and precise control over band gap distances.

Table 1Drude model fit calculated relative DC Conductivities of all samples.

Relative Colludictivities (3/Cili)
6 wt% CaTiO ₃ : PVDF = 1.8×10^{-3}
9 wt% CaTiO ₃ : PVDF = 5.1×10^{-3}
37 wt% CaTiO ₃ : PVDF = 12.8×10^{-3}
6 wt% LiNbO ₃ : PVDF = 1.5×10^{-3}
9 wt% LiNbO ₃ : PVDF = 1.3×10^{-3}
38 wt% LiNbO ₃ : PVDF = 1.1×10^{-3}
35 um PVDF = 9.0×10^{-4}
71 um PVDF = 1.8×10^{-3}
140 um PVDF = 2.0×10^{-3}

Polotico Conductivitios (C/om)

The implications of our study lay a solid foundation for the innovative design of materials with customizable properties. By unraveling the intricate effects of dopant integration within the PVDF matrix, this work not only contributes significantly to the field of composite materials but also paves the way for groundbreaking advancements in organic electronics.

In essence, this study offers a comprehensive framework for the targeted development of advanced materials. By drawing connections between the fundamental properties of $CaTiO_3$ and $LiNbO_3$ crystals and the enhanced capabilities of PVDF composites, we underscore the immense potential for engineering materials that can meet the evolving demands of modern technology. Through this work, we will further explore into the dynamics and mechanisms of conductivity enhancement of crystal-doped polymers, anticipating new pathways leveraging innovative techniques, that will undoubtedly lead to novel technological innovations.

CRediT authorship contribution statement

Clyde Varner: Writing – review & editing, Writing – original draft, Visualization, Validation, Supervision, Software, Resources,

Methodology, Investigation, Formal analysis, Data curation, Conceptualization. **Angela Davis:** Writing – review & editing, Writing – original draft, Visualization, Data curation. **Ashok K. Batra:** Conceptualization. **Padmaja Guggilla:** Investigation.

Declaration of competing interest

The authors declare that they have no known competing financial interests or personal relationships that could have appeared to influence the work reported in this paper.

Data availability

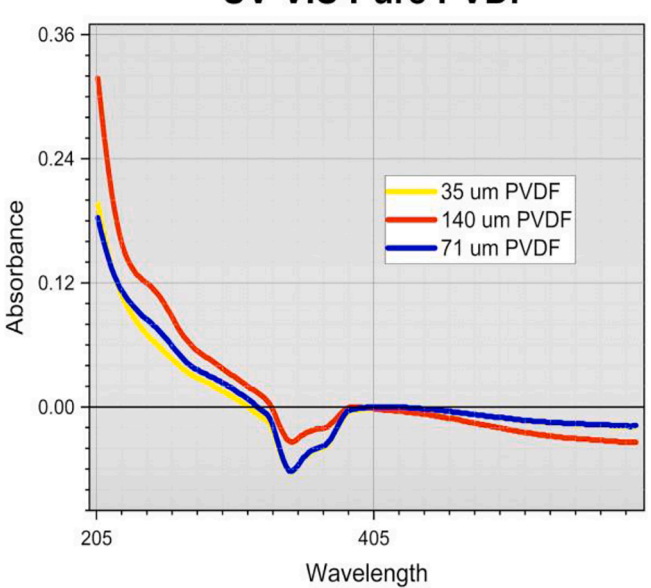
Data will be made available on request.

Acknowledgements

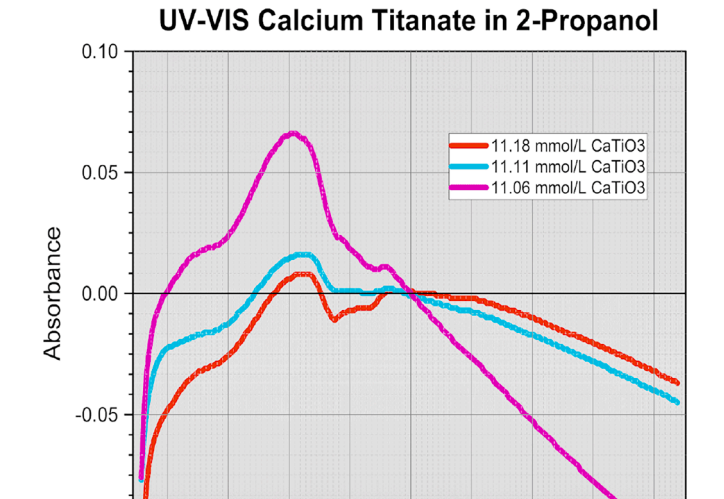
This work was supported by the National Science Foundation under Grant No. # 2331969. Any opinions, findings, and conclusions or recommendations expressed in this work are those of the author(s) and do not necessarily reflect the views of the National Science Foundation.

Appendices.

UV-VIS Pure PVDF



A1. UV-Vis Spectrum of Pure PVDF



A2. UV Vis spectru if CaTiO3 Nanocrystals in 2- Propanol

357

401

Wavelength

445

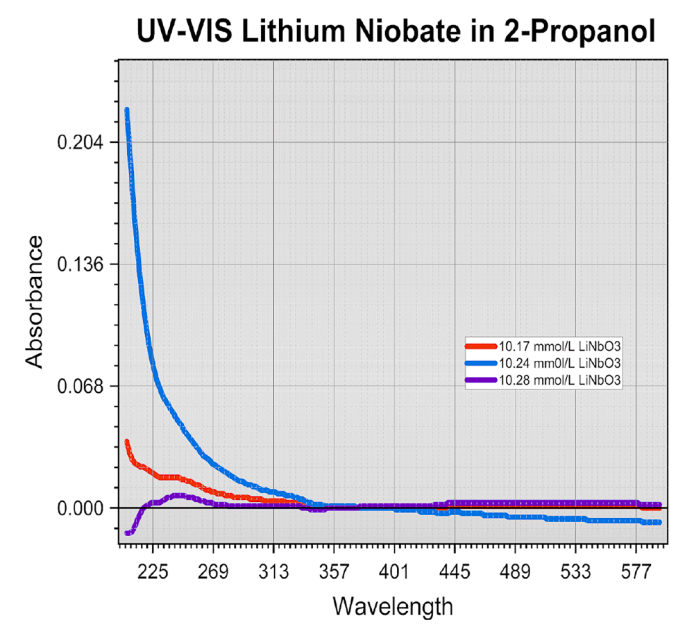
489

533

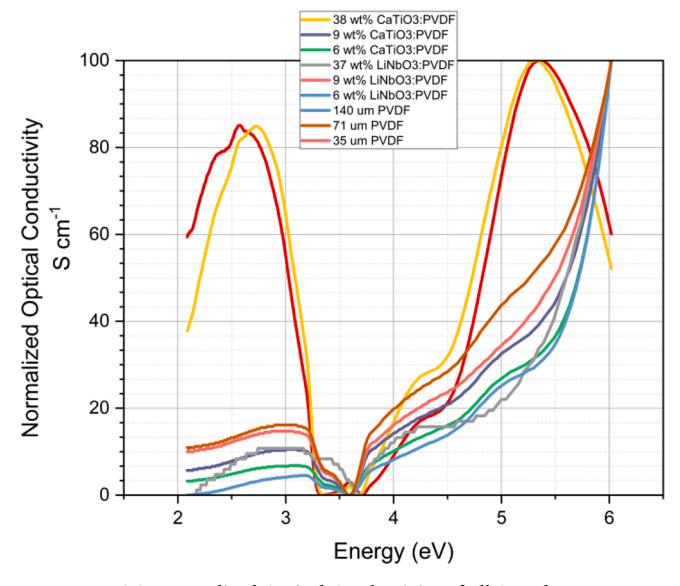
-0.10

269

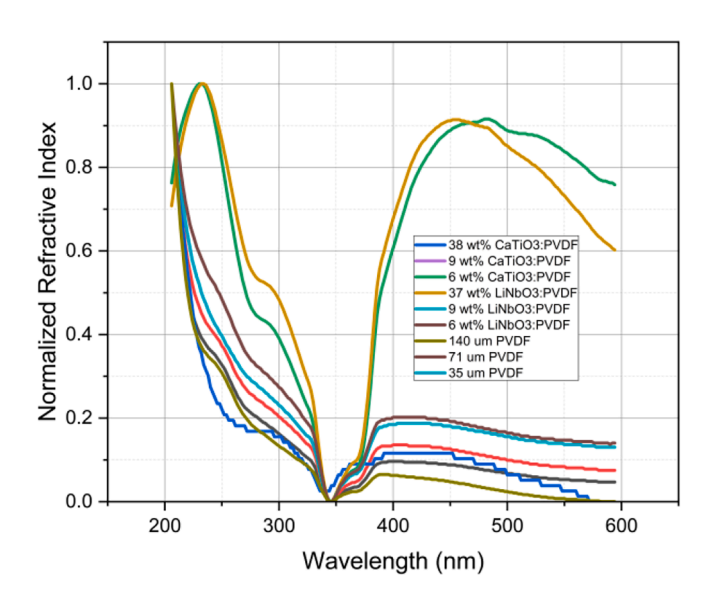
313



A3. UV Vis spectru if LiNbO3 Nanocrystals in 2- Propanol



A4. Normalized Optical Conductivity of all Samples



A5. Normalized Refractive Index of all Samples

References

Abbas, S.S., Raouf, R.M., Al-Moameri, H.H., 2023. Preparation of calcium titanate nanoparticles with investigate the thermal and electrical properties by incorporating epoxy. Mater. Sci. Forum 1083, 13–22.

Acikgoz, M., Mollabashi, L., Rahimi, S., Jalali-Asadabadi, S., Rudowicz, C., 2023. DFT computations combined with semiempirical modeling of variations with temperature of spectroscopic and magnetic properties of Gd³⁺-doped PbTiO₃. PCCP 25, 3986–4004.

Advanced Materials for Solid State Lighting. vol. 25, Springer Nature Singapore, Singapore, 2023.

Cerda-Sumbarda, Y.D., Zizumbo-Lopez, A., Licea-Claverie, A., 2023. Nanomaterials. In: Phytochemical Nanodelivery Systems as Potential Biopharmaceuticals. Elsevier, pp. 71–122. https://doi.org/10.1016/B978-0-323-90390-5.00008-6.

Chahar, S., Mishra, K.K., Sharma, R., 2024. Analysing the suitability of CaTiO3/ Ca1-xSrxTiO3/SrTiO3 perovskite for fabrication of optoelectronic devices using QuantumATK tool: a study for electronic and optical properties. Phys. Scr. 99, 35963.

Chaibi, N., Hemmouche, L., Trache, D., Benkhelil, H., Hedimi, H., 2021. Study of the influence of nanoparticles on the behavior of composite materials. J. Indian Chem. Soc. 98, 100151. Dilshod, N., et al., 2022. On the optical properties of the Cu2ZnSn[S1-xSex]4 system in the IR range. Trends Sci. 20, 4058.

Jilani, W., Jlali, A., Guermazi, H., 2021. Impact of CuO nanofiller on structural, optical and dielectric properties of CuO/DGEBA hybrid nanocomposites for optoelectronic devices. Opt. Quant. Electron. 53, 545.

Kumar, S., et al., 2023. Advantages and disadvantages of metal nanoparticles. In: Nanoparticles Reinforced Metal Nanocomposites. Springer Nature Singapore, Singapore, pp. 209–235. https://doi.org/10.1007/978-981-19-9729-7_7.

Kunwar, D., Vazquez, I.R., Jackson, N., 2022. Effects of solvents on synthesis of piezoelectric polyvinylidene fluoride trifluoroethylene thin films. Thin Solid Films 757, 139414.

Makula, P., Pacia, M., Macyk, W., 2018. How to correctly determine the band gap energy of modified semiconductor photocatalysts based on UV–Vis spectra. J. Phys. Chem. Lett. 9, 6814–6817.

Mallick, P., Satpathy, S.K., Moharana, S., 2023. Nanomaterials for fabrication of thermomechanical robust composite. In: Nanoparticles Reinforced Metal Nanocomposites. Springer Nature Singapore, Singapore, pp. 297–315. https://doi. org/10.1007/978-981-19-9729-7 10.

Mayou, D., 2000. Generalized drude formula for the optical conductivity of quasicrystals. Phys. Rev. Lett. 85, 1290–1293.

Laser Synthesis of Nanomaterials. (MDPI, 2023). doi: 10.3390/books978-3-0365-6928-4.

- Mehra, R.M., 2022. Electronic and mechanical properties of nanoparticles. In: Applications of Nanomaterials for Energy Storage Devices. CRC Press, Boca Raton, pp. 127–141. https://doi.org/10.1201/9781003216308-6.
- Neagu, R.M., Neagu, E., Bonanos, N., Pissis, P., 2000. Electrical conductivity studies in nylon 11. J. Appl. Phys. 88, 6669–6677.
- Novruzova, A.A., 2021. Structure and electrophysical properties of PVDF+PbS/CdS Nanocomposites. NNC RK Bullet. 53–56 https://doi.org/10.52676/1729-7885-2021-2-53-56.
- Omeiza, L.A., et al., 2023. Nanostructured electrocatalysts for advanced applications in fuel cells. Energies (Basel) 16, 1876.
- Ostlind, A., et al., 2022. Scalable synthesis of a bulk nanocrystalline material with a multitude of divergent properties through a traditional manufacturing process. Mater. Today Commun. 33, 104390.
- Panda, S., et al., 2022. Biocompatible CaTiO3-PVDF composite-based piezoelectric nanogenerator for exercise evaluation and energy harvesting. Nano Energy 102, 107682
- Qahtan, A.A.A., Husain, S., Khan, W., 2021. The effect of Ni doping on the structural, optical and dielectric properties of nanocrystalline YbCrO3. J. Phys. Chem. Solid 159, 110280
- Synak, A., et al., 2022. New core-shell nanostructures for FRET studies: synthesis, characterization, and quantitative analysis. Int. J. Mol. Sci. 23, 3182.
- Tabhane, G., Giripunje, Sushama, M., Kondawar, S.B., 2022. ${\rm CuO/ZnO/Ni_2O_3}$ ternary nanocomposite encapsulated BaTiO $_3$ /PVDF for high energy storage density. In: 2022 International Conference on Electrical, Computer, Communications and

- Mechatronics Engineering (ICECCME). IEEE, pp. 1–6. https://doi.org/10.1109/ICECCME55909.2022.9988262.
- Tan, C., et al., 2022. Hydrogenated boron phosphide THz-metamaterial-based biosensor for diagnosing COVID-19: a DFT coupled FEM study. Nanomaterials 12, 4024. Uličná, S., et al., 2022. A study of degradation mechanisms in PVDF-based photovoltaic
- Wang, X., Qiao, B., Tan, S., Zhu, W., Zhang, Z., 2020. Tuning the ferroelectric phase transition of PVDF by uniaxially stretching crosslinked PVDF films with CF=CH bonds. J. Mater. Chem. C 8, 11426–11440.

backsheets. Sci. Rep. 12, 14399.

- Wenzhong Ma Jun Zhang, S.C., Wang, X., 2008. Crystalline phase formation of poly (vinylidene fluoride) from tetrahydrofuran/N, N-dimethylformamide mixed solutions. J. Macromol. Sci., Part B 47, 434–449.
- Wu, Y.-C., Tseng, H.-T., Hsi, C.-S., Juuti, J., Hsiang, H.-I., 2022. Low dielectric loss ceramics in the Mg4Nb2O9-ZnAl2O4-TiO2 ternary system. J. Eur. Ceram. Soc. 42, 449, 452
- Xu, P., Fu, W., Luo, X., Ding, Y., 2017. Enhanced dc conductivity and conductivity relaxation in PVDF/ionic liquid composites. Mater. Lett. 206, 60–63.
- Zhang, C., et al., 2023. Enhanced energy storage performance of doped modified PC/ PVDF coblended flexible composite films. ACS Appl. Electron. Mater. 5, 3817–3829.
- Zhou, Y., et al., 2021. Crystallinity and β phase fraction of PVDF in biaxially stretched PVDF/PMMA Films. Polymers (Basel) 13.
- Zhou, X., Cakmak, M., 2007. Phase behavior of rapidly quenched PVDF/PMMA blends as characterized by Raman spectroscopy, X-ray diffraction and thermal techniques. J. Macromol. Sci., Part B 46, 667–682.